Analytical Study of Dynamic Response of Railway on Partial Elastic Foundation under Travelling Accelerating Concentrated Load

Amin Ghannadiasl[1]

Received: 17.02.2016 *Accepted: 01.02.2017*

Abstract

The dynamic response of the railway under accelerated moving load using Dynamic Green Function is presented in this paper. For this purpose, an exact and direct modeling technique is introduced for the railway modeling as the damped Euler-Bernoulli beam on the partial Winkler foundation with arbitrary boundary conditions subjected to the moving load. The effects of the elastic coefficient of Winkler foundation, as well as velocity and accelerate of the moving load are assessed. The results are shown that the maximum deflection depends on the increasing or decreasing acceleration of the moving load. On the other hands, it does not occur at the central point of the beam for all acceleration values. Based on the results, the acceleration value of load dominantly defines the dynamic deflection shape of the Euler-Bernoulli beam. Some numerical examples are shown to demonstrate the simplicity and efficiency of the Dynamic Green Function in the new formulation, in this paper.

Keywords: Damped Euler-Bernoulli beam, Dynamic Green Function, moving load and boundary conditions

Corresponding author E-mail: aghannadiasl@uma.ac.ir

[1] Assistant Professor, Faculty of Engineering, University of Mohaghegh Ardabili, Ardabil, Iran.

1. Introduction

The dynamic effects of moving loads were not noticed until the mid-19th century. Ting et al. developed the double Laplace transformation method to solve the dynamic analysis of the damped Euler–Bernoulli beam under a moving concentrated force [Hamada, 1981]. Mackertich provided the dynamic response of the simply supported Timoshenko beam under the moving load [Mackertich, 1990]. Lin investigated the dynamic analysis of Timoshenko beam under moving load using finite element method [Lin, 1994]. In that research, the rotary inertia and shear effect are considered and the modal superposition is used to solve system equations. Hilal and Zibdeh presented the vibration of Euler–Bernoulli beam with general boundary conditions under the moving load as closed-form solutions [Hilal and Zibdeh, 2000]. Savin formulated an analytical expression of the dynamic amplification factor for the Euler–Bernoulli beam under the successive moving loads [Savin, 2001]. A method for determining the dynamic response of Euler–Bernoulli beam under the concentrated and distributed loads is presented by Abu-Hilal [Abu-Hilal, 2003]. It is used to solve single and multi-loaded beams, single and multi-span beams, and statically determinate and indeterminate beams. Furthermore, the response of the uniform Timoshenko beam with infinite length on Pasternak-type viscoelastic foundation under the harmonic moving load studied by Kargarnovin and Younesian [Kargarnovin and Younesian, 2004]. The governing differential equations solve using complex Fourier transformation in conjunction with the residue and convolution integral theorems.

Mehri et al. presented the dynamic response of a uniform Euler–Bernoulli beam under moving load by the Dynamic Green Function [Mehri et al., 2009]. The spectral analysis of beam under a random train of moving force is offered by Gładysz and Śniady [Gładysz and Śniady, 2009]. Koziol and Mares exhibited the response of a solid forced by a fast moving load [Koziol and Mares, 2010]. In this study, the mathematical model is described by the Euler-Bernoulli equation for the beam and the Navier's elasto-dynamic equation for the soil. Beskou and Theodorakopoulos presented a comprehensive review on the subject of the dynamic response of pavement structures under moving loads [Beskou and Theodorakopoulos, 2011]. Also, Ouyang provided an extensively advantageous overview of structural dynamics problems caused by moving loads [Ouyang, 2011]. Bajer and Dyniewicz exhibited broad description of numerical tools successfully applied to the dynamic analysis of the structures under moving inertial load [Bajer and Dyniewicz, 2012]. Dimitrovová and Rodrigues investigated the analysis of the critical velocity of moving load along an Euler-Bernoulli beam on the viscoelastic foundation [Dimitrovová and Rodrigues, 2012]. The critical velocity is defined as the load velocity inducing the beam's highest deflections. Zrnić et al. presented a combined finite element and analytical method for obtaining vibration of a gantry crane system under an elastically suspended moving body [Zrnić et al., 2015]. The dynamic analysis of the axially Euler–Bernoulli beam on Visco-elastic foundation under moving load is presented Mohammadzadeh and Mosayebi [Mohammadzadeh and Mosayebi, 2014]. Zakeri and Shahbabaei introduced effect of elastic supports stiffness on the natural frequencies and modes of two span beams [Zakeri and Shahbabaei, 2015]. Dimitrovová derived a new formula for the critical velocity of the moving load [Dimitrovová, 2016]. It is considered that the Euler–Bernoulli beam supported by a foundation with a finite depth. Also, a mathematical model of the vehicle–floating slab track interaction to investigate the coupled behavior of the vehicle–track system is presented by Esmaeili et al. [Esmaeili et al., 2016].

In the previous studies, the dynamic analysis of the undamped Euler–Bernoulli beam under the accelerated moving load is presented using the Dynamic Green Function. On the other hands, these solutions cannot be generalized to arbitrary boundary conditions for damped Euler–Bernoulli beam on a partial Winkler foundation under accelerated moving load. Therefore, the objectives of this paper are:

- To present an analytical–numerical technique for the dynamic response of damped Euler–Bernoulli beams, with arbitrary boundary conditions, on the partial Winkler foundation under accelerated moving load.

- To state an exact solution in closed form using the Dynamic Green Function.

2. Modeling of Beam on Winkler Foundation under Accelerating Moving Load

In this paper, it is assumed a damped Euler–Bernoulli beam under accelerating moving load on the partial Winkler foundation as shown in Figure 1. By applying Hamilton's principle, the differential equation of motion for the transverse displacement of the damped Euler–Bernoulli beam with uniformly distributed external damping and simple model of internal damping (Kelvin-Voigt model) can be determined by:

$$\begin{aligned} EI\, w_{,xxxx} + r_i w_{,xxxxt} + r_e w_{,t} + \rho A\, w_{,tt} & \\ + K_W w\big(H(x-\beta_L L) & \\ - H(x-(\beta_L+\beta_L)L)\big) & \\ = F\,\delta\big(x-\mathrm{X_F(t)}\big) & \end{aligned} \quad (1)$$

where $w(x,t)$ is the transverse deflection of the mid-surface of the beam and F is the concentrated force exerted by the moving load on the beam. In addition, I, E, r_i, r_e, A and ρ are the second moment of area, the Young's modulus of elasticity, the internal damping coefficient of the beam that is generally very small [Lancaster and Shkalikov, 1994], the external damping coefficient of the beam, the cross-sectional area of the beam, and the beam material density, respectively. Also, $H(w)$ is the Heaviside unit function which is defined as:

$$H(x-u) = \begin{cases} 0, & x < u \\ 1, & x > u \end{cases} \quad (2)$$

In this paper, the internal and external damping effects are assumed to be proportional to the stiffness properties and mass of the Euler–Bernoulli beam, respectively. These characteristics are assumed as [Hilal and Zibdeh, 2000]:

$$r_i = \alpha_i EI \quad (3)$$

$$r_e = \alpha_e \rho A \quad (4)$$

where α_i and α_e are the proportionality constants. The dimensionless damping ratio of the n^{th} mode of the uniform Euler-Bernoulli beam with internal damping can be represented as:

$$\xi_i = \frac{1}{2}\alpha_i\omega_n \quad (5)$$

where ω_n is the n^{th} natural frequency of the undamped Euler-Bernoulli beam. The dimensionless damping ratio of the n^{th} mode of the uniform beam with external damping can be given by:

$$\xi_e = \frac{1}{2}\frac{\alpha_e}{\omega_n} \quad (6)$$

Therefore, the damping factor diminishes in the uniform beam with external damping at higher modes. On the other hands, the Dirac Delta function (δ) is defined by:

$$\delta(x-X) = \begin{cases} +\infty & if\ x = X \\ 0 & if\ x \neq X \end{cases} \quad (7)$$

The equation of the trajectory of the moving load, $\mathrm{X_F(t)}$, is defined as:

$$X_F(t) = v_{0x}t + \tfrac{1}{2}a_{0x}t^2 \quad (8)$$

where v_{0x} is the initial speed of the moving load in the x direction and a_{0x} is the constant acceleration of the moving load in the x direction. This function can be described a uniform accelerating or decelerating motion. In the paper, the homogeneous initial conditions associated with the damped Euler–Bernoulli beam theory are given below:

$$w(x,0) = 0 \qquad w_{,t}(x,0) = 0 \quad (9)$$

$$\theta(x,0) = 0 \qquad \theta_{,t}(x,0) = 0 \quad (10)$$

where $w(x,t)$ and $\theta(x,t)$ are the transverse deflection of the mid-surface of the beam and anticlockwise angle of rotation of the normal to the mid-surface, respectively. It is noted that each function $w(x,t)$ can be presented in the form of a product of a function dependent on the coordinate x and a function dependent on the time t:

$$w(x,t) = W(x)\,T(t) \quad (11)$$

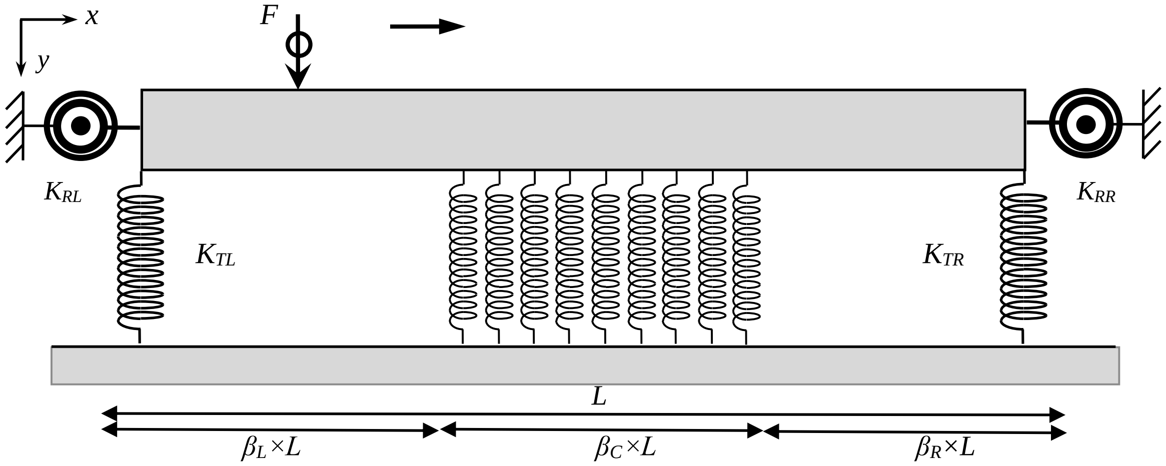

Figure 1. Schematic description of damped Euler–Bernoulli beam on the partial Winkler foundation under accelerating moving load

where $W(\mathrm{x})$ is the mid-surface deflection in point x of the Euler–Bernoulli beam. The Dynamic Green Function is utilized to find the solution of equation (1) [Li et al., 2014; Mehri et al., 2009]. Hence, if $\mathrm{G}(\mathrm{x}, X_F)$ is the Dynamic Green Function of the submitted problem for a concentrated moving load, the solution of equation (1) can be presented the form

$$w(x,t) = F\,G(x, X_F) \tag{12}$$

Therefore, the Dynamic Green Function for a moving load, $G(x, \mathrm{X}_F)$, is the solution of the differential equation:

$$\left(1 + \frac{r_i}{EI} i\omega\right) G_{,xxxx} + \frac{1}{EI}\left(r_e i\omega - \rho A\omega^2 + K_W\right) G = \frac{1}{EI}\,\delta\big(x - X_F(t)\big) \tag{13}$$

where ω is the circular frequency of the concentrated moving load. The circular frequency of the moving load is calculated as:

$$\omega = \frac{\pi\, v}{L} \tag{14}$$

where v is the speed of the concentrated moving load in the x direction. The speed of the moving load is given as:

$$v = \sqrt{{v_{0x}}^2 + 2\, a_{0x}\, X_F} \tag{15}$$

The general solution of the differential equation (13) can be stated as equation (16):

where $x \in [0, L]$ and i represents the imaginary unit $\sqrt{-1}$. The parameter λ is calculated as:

$$\lambda = \sqrt[4]{\frac{\phi^2\left(1 - 2i\frac{\xi_e}{\beta_n}\right) - \eta}{1 + 2i\xi_i\beta_n}} \tag{17}$$

$$G(x, X_F) = \begin{cases} C_1 \sin(\lambda x) + C_2 \cos(\lambda x) + C_3 \sinh(\lambda x) + C_4 \cosh(\lambda x) & 0 \le x \le X_F \\ C_5 \sin(\lambda x) + C_6 \cos(\lambda x) + C_7 \sinh(\lambda x) + C_8 \cosh(\lambda x) & \\ \quad + \dfrac{\sin(\lambda(X_F - x)) - \sinh(\lambda(X_F - x))}{2\lambda^3 EI(1 + 2i\xi_i\beta_n)} & X_F \le x \le L \end{cases} \tag{16}$$

where ϕ is the parameter proportional to the forcing frequency ($\phi^2 = \frac{\omega^2 \rho A}{EI}$), β_n, the parameter proportional to the frequency ratio that is given as the ratio of the forcing frequency to the natural frequency of beam. ($\beta_n = \frac{\omega}{\omega_n}$), ξ_i, the damping ratio proportional to the internal damping $\left(\xi_i = \frac{1}{2}\alpha_i \omega_n\right)$, ξ_e, the damping ratio proportional to the external damping $\left(\xi_e = \frac{1}{2}\frac{\alpha_e}{\omega_n}\right)$, and η is the parameter proportional to the elastic coefficient of Winkler foundation $\left(\eta = \frac{K_W}{EI}\right)$. In equation (16), $C_1, \ldots, C_7$ and C_8 are the integration constants that are evaluated such that the Dynamic Green Function satisfies two boundary conditions at each end of the beam depending on the type of end support included. In this paper, the general boundary conditions associated with the Euler–Bernoulli beam theory are given below [Abu-Hilal, 2003]:

$$V(0, X_F) = -K_{TL}\, w(0, X_F) \tag{18}$$

$$M(0, X_F) = K_{RL}\, \theta(0, X_F) \tag{19}$$

$$V(L, X_F) = K_{TR}\, w(L, X_F) \tag{20}$$

$$M(L, X_F) = -K_{RR}\, \theta(L, X_F) \tag{21}$$

where M, V and θ are the bending moment ($M = EI\, w_{,xx}$), the shear force ($V = EIw_{,xxx}$), and slope ($\theta = w_{,x}$), respectively [Wang, 1995]. The Green Function for the Euler–Bernoulli beam under concentrated moving load obtained by the above procedure, has a general form. By applying the relationships between the individual physical quantities and the Green Function, the jump condition and the continuity conditions at $x = X_F$ can be written as the following [Ghannadiasl and Mofid, 2014, 2015]:

$$G(X_F^+, X_F) - G(X_F^-, X_F) = 0 \tag{22a}$$

$$G_{,x}(X_F^+, X_F) - G_{,x}(X_F^-, X_F) = 0 \tag{22b}$$

$$G_{,xx}(X_F^+, X_F) - G_{,xx}(X_F^-, X_F) = 0 \tag{22c}$$

$$G_{,xxx}(X_F^+, X_F) - G_{,xxx}(X_F^-, X_F) = \frac{1}{EI(1 + 2i\xi_i\beta_n)} \tag{22d}$$

Therefore, the Dynamic Green Function for the damped Euler–Bernoulli beam on the uniform Winkler foundation ($\beta_R = \beta_L = 0$ and $\beta_C = 1$) under the accelerated moving load where it is partially restrained against translation and rotation at its ends ($K_{RR} = K_{RL} = K_R$ and $K_{TR} = K_{TL} = K_T$) is given below:

$$G(x, X_F) = \frac{1}{2EI\lambda^3(1 + 2i\xi_i\beta_n)B_3} \begin{cases} g(x, X_F) & 0 \le x \le X_F \\ g(X_F, x) & X_F \le x \le L \end{cases} \tag{23}$$

$$g(x, X_F) = D_1 \sin(\lambda x) + D_2 \cos(\lambda x) + D_3 \sinh(\lambda x) + D_4 \cosh(\lambda x)$$

$$\begin{aligned} D_1 = {} & 2\frac{K_T}{EI}\lambda\left(\lambda^3 \cos\big(\lambda(L - X_F)\big) + \lambda^3 \cosh\big(\lambda(L - X_F)\big) + \frac{K_T}{EI}\sin\big(\lambda(L - X_F)\big)\right. \\ & \left. - \frac{K_T}{EI}\sinh\big(\lambda(L - X_F)\big)\right)\left(2\frac{K_T}{EI}\lambda\left(\frac{K_R}{EI}\cosh(\lambda L) + \lambda \sinh(\lambda L)\right)\right. \\ & \left. + \left(\lambda \cosh(\lambda L) + \frac{K_R}{EI}\sinh(\lambda L)\right)B_1 + \left(\lambda \cos(\lambda L) + \frac{K_R}{EI}\sin(\lambda L)\right)B_2\right) \\ & + \left(\frac{K_R}{EI}\cos\big(\lambda(L - X_F)\big) - \frac{K_R}{EI}\cosh\big(\lambda(L - X_F)\big) - \lambda \sin\big(\lambda(L - X_F)\big)\right. \\ & \left. - \lambda \sinh\big(\lambda(L - X_F)\big)\right)\left(2\frac{K_T}{EI}\lambda\left(\lambda^3 \cosh(\lambda L) - \frac{K_T}{EI}\sinh(\lambda L)\right)\right. \\ & \left. + \left(-\frac{K_T}{EI}\cosh(\lambda L) + \lambda^3 \sinh(\lambda L)\right)B_1 + \left(\frac{K_T}{EI}\cos(\lambda L) + \lambda^3 \sin(\lambda L)\right)B_2\right) \end{aligned}$$

$$D_2 = -B_1 \frac{D_1}{2\lambda \frac{K_T}{EI}} - B_2 \frac{D_3}{2\lambda \frac{K_T}{EI}}$$

$$\begin{aligned} D_3 = -2\frac{K_T}{EI}\lambda \Bigg(& 2\frac{K_T}{EI}\lambda \Big(cosh\big(\lambda(L - X_F)\big) \Big(2\frac{K_R}{EI}\lambda^3 cos(\lambda L) + B_1 sin(\lambda L) \Big) - B_2 sin(\lambda X_F) \\ & + sinh\big(\lambda(L - X_F)\big) \Big(-B_1 cos(\lambda L) + 2\frac{K_T}{EI}\lambda sin(\lambda L) \Big) \Big) \\ & + B_1 \Big(B_2 cos(\lambda X_F) + cosh\big(\lambda(L - X_F)\big) \Big(-B_1 cos(\lambda L) + 2\frac{K_R}{EI}\lambda^3 sin(\lambda L) \Big) \\ & - sinh\big(\lambda(L - X_F)\big) \Big(2\frac{K_T}{EI}\lambda cos(\lambda L) + B_1 sin(\lambda L) \Big) \Big) \\ & + B_2 \Big(B_2 cosh(\lambda X_F) + cos\big(\lambda(L - X_F)\big) \Big(-B_1 cosh(\lambda L) + 2\frac{K_R}{EI}\lambda^3 sinh(\lambda L) \Big) \Big) \\ & + sinh\big(\lambda(L - X_F)\big) \Big(-2\frac{K_T}{EI}\lambda cosh(\lambda L) + B_1 sinh(\lambda L) \Big) \Big) \end{aligned}$$

$$D_4 = B_2 \frac{D_1}{2\lambda \frac{K_T}{EI}} + B_1 \frac{D_3}{2\lambda \frac{K_T}{EI}}$$

$$B_1 = \frac{K_R}{EI}\frac{K_T}{EI} - \lambda^4$$

$$B_2 = \frac{K_R}{EI}\frac{K_T}{EI} + \lambda^4$$

$$\begin{aligned} B_3 = cos(\lambda L) \Bigg(& B_1 sinh(\lambda L) \left(8\frac{K_T}{EI}\lambda^2 \left(\frac{K_R}{EI}\lambda^2 - \frac{K_T}{EI} \right) \right) - 4\frac{K_T}{EI}\lambda cosh(\lambda L) \left({B_1}^2 - 4\frac{K_T}{EI}\frac{K_R}{EI}\lambda^2 \right) \Bigg) \\ & + sin(\lambda L) \Bigg(B_1 cosh(\lambda L) \left(8\frac{K_T}{EI}\lambda^2 \left(\frac{K_R}{EI}\lambda^2 + \frac{K_T}{EI} \right) \right) + 8\lambda^3 sinh(\lambda L) \left(\left(\frac{K_T}{EI} \right)^3 - \frac{K_T}{EI}\left(\frac{K_R}{EI} \right)^2 \lambda^4 \right) \Bigg) \\ & + 4\frac{K_T}{EI}\lambda {B_2}^2 \end{aligned}$$

where, $g(X_F, x)$ is obtained by switching x and X_F in $g(x, X_F)$. This follows from the fact that $G(x, X_F)$ must be symmetric to satisfy the Maxwell-Rayleigh reciprocity law. For example, in the damped Euler–Bernoulli beam, the Dynamic Green Function for the simply supported boundary condition is given below:

The expression given by equation (24) is exactly the forced vibration part obtained by Abu-Hilal [Abu-Hilal, 2003]. In this paper, the Euler–Bernoulli beam divides into three segments with and without Winkler foundation.

$$G(x, X_M) = \frac{1}{2\,EI\,\left(1 + 2i\xi_i\beta_n\right)\lambda^3} \begin{cases} g(x, X_F) & 0 \le x \le X_F \\ g(X_F, x) & X_F \le x \le L \end{cases} \tag{24}$$

$$g(x, X_F) = \frac{sin\big(\lambda(L - X_F)\big)}{sin(\lambda L)} sin(\lambda x) - \frac{sinh(\lambda(L - X_F))}{sinh(\lambda L)} sinh(\lambda x)$$

$$G_L(x,X_F)=\begin{cases} C_{1L}\,sin(\lambda_L x)+C_{2L}\,cos(\lambda_L x)+C_{3L}\,sinh(\lambda_L x)+C_{4L}\,cosh(\lambda_L x) & 0\le x\le X_F \\ C_{5L}\,sin(\lambda_L x)+C_{6L}\,cos(\lambda_L x)+C_{7L}\,sinh(\lambda_L x)+C_{8L}\,cosh(\lambda_L x) \\ \quad +\dfrac{sin(\lambda_L(X_F-x))-sinh(\lambda_L(X_F-x))}{2{\lambda_L}^3EI(1+2i\xi_i\beta_n)} & X_F\le x\le \beta_L L \end{cases} \tag{25}$$

$$G_C(x,X_F)=\begin{cases} C_{1C}\,sin(\lambda_C x)+C_{2C}\,cos(\lambda_C x)+C_{3C}\,sinh(\lambda_C x)+C_{4C}\,cosh(\lambda_C x) & \beta_L L\le x\le X_F \\ C_{5C}\,sin(\lambda_C x)+C_{6C}\,cos(\lambda_C x)+C_{7C}\,sinh(\lambda_C x)+C_{8C}\,cosh(\lambda_C x) \\ \quad +\dfrac{sin(\lambda_C(X_F-x))-sinh(\lambda_C(X_F-x))}{2{\lambda_C}^3EI(1+2i\xi_i\beta_n)} & X_F\le x\le L(\beta_L+\beta_C) \end{cases} \tag{26}$$

$$G_R(x,X_F)=\begin{cases} C_{1R}\,sin(\lambda_R x)+C_{2R}\,cos(\lambda_R x)+C_{3R}\,sinh(\lambda_R x)+C_{4R}\,cosh(\lambda_R x) & L(\beta_L+\beta_C)\le x\le X_F \\ C_{5R}\,sin(\lambda_R x)+C_{6R}\,cos(\lambda_R x)+C_{7R}\,sinh(\lambda_R x)+C_{8R}\,cosh(\lambda_R x) \\ \quad +\dfrac{sin(\lambda_R(X_F-x))-sinh(\lambda_R(X_F-x))}{2{\lambda_R}^3EI(1+2i\xi_i\beta_n)} & X_F\le x\le L \end{cases} \tag{27}$$

The differential equation of the vibration can be presented for each segment. Therefore, the Dynamic Green Function for the first segment can be stated as equation (25), where $x\in[0,\beta_L L]$, λ_L is calculated as:

$$\lambda_L=\sqrt[4]{\frac{\phi^2\left(1-2i\frac{\xi_e}{\beta_n}\right)}{1+2i\xi_i\beta_n}} \tag{28}$$

For the middle section, the Dynamic Green Function takes the form of equation (26), where $x\in(\beta_L L, L(\beta_L+\beta_C)]$, λ_C is calculated as:

$$\lambda_C=\sqrt[4]{\frac{\phi^2\left(1-2i\frac{\xi_e}{\beta_n}\right)-\eta}{1+2i\xi_i\beta_n}} \tag{29}$$

Similarly, it is possible to develop the Dynamic Green Function for the last section of the Euler–Bernoulli beam (equation (27)), where $x\in(L(\beta_L+\beta_C), L]$, λ_R is calculated as:

$$\lambda_R=\sqrt[4]{\frac{\phi^2\left(1-2i\frac{\xi_e}{\beta_n}\right)}{1+2i\xi_i\beta_n}} \tag{30}$$

$C_{1L}-C_{8L}$, $C_{1C}-C_{8C}$ and $C_{1R}-C_{8R}$ are the constant unknowns of the three above-mentioned solutions. In order to find these unknowns, it is required to develop twenty-four equations.

$$W_d(x,X_F) = -\frac{F\,v}{2EI\lambda^2\omega_n(1+2i\xi_i\beta_n)}\sin\left(\frac{\omega_n}{v}X_F\right)\left(\frac{\sin(\lambda(L-x))}{\sin(\lambda L)} - \frac{\sinh(\lambda(L-x))}{\sinh(\lambda L)}\right) \quad (33)$$

$$0 \le x, X_F \le L$$

The constant unknowns are obtained using two boundary conditions at each end of the beam depending on the type of end support and the continuity conditions of slope, displacement and moment along with the shear force in the vicinities of the different segment connections. The continuity conditions are defined as:

$$G_L(\beta_L L) = G_C(\beta_L L) \quad (31a)$$

$$\theta_L(\beta_L L) = \theta_C(\beta_L L) \quad (31b)$$

$$M_L(\beta_L L) = M_C(\beta_L L) \quad (31c)$$

$$V_L(\beta_L L) = V_C(\beta_L L) \quad (31d)$$

and

$$G_C(\beta_L L + \beta_C L) = G_R(\beta_L L + \beta_C L) \quad (32a)$$

$$\theta_C(\beta_L L + \beta_C L) = \theta_R(\beta_L L + \beta_C L) \quad (32b)$$

$$M_C(\beta_L L + \beta_C L) = M_R(\beta_L L + \beta_C L) \quad (32c)$$

$$V_C(\beta_L L + \beta_C L) = V_R(\beta_L L + \beta_C L) \quad (32d)$$

Equations (23) and (24) are presented the particular solution for the governing equation (the forced vibration part of the deflection) of the stated problem. The boundary conditions are embedded in the Dynamic Green function for equations (23) and (24). Although, it still needs to satisfy the two initial conditions given by equations (9) and (10). Therefore, the complementary solution should be added for equations (23) that is given by equation (33), where ω_n is the nth natural frequency of Euler–Bernoulli beam and v is the speed of the load ($v = v_{0x} + a_{0x}t$). The dimensionless speed parameter is defined as:

$$\alpha = \frac{v}{v_{cr}} = \frac{v_{0x} + a_{0x}t}{v_{cr}} \quad (34)$$

where, v_{cr}, the critical speed is equal by $v_{cr} = \frac{2L}{T} = \frac{L}{\pi}\omega_n$.

3. Numerical Examples

For the purpose of verification, a simply supported Euler–Bernoulli beam neglecting the damping effect of the beam subjected to a moving load is considered. The beam is supposed with the following characteristics:

$K_W = 0 \qquad \xi_e = 0 \quad \xi_i = 0$

$\phi^2 = \frac{\omega^2 \rho A}{EI} \qquad v = \alpha\, v_{cr} \qquad X_F(t) = v_{0x}t$

$\omega = \frac{\pi v}{L} \qquad a_{0x} = 0$

For the simply supported damping Euler–Bernoulli beam, the nth damped natural frequency is:

$$\omega_{nD} = i\omega_n\left(\xi \pm \sqrt{\xi^2 - 1}\right) \quad (35)$$

where ω_n is the nth undamped natural frequency of the simply supported Euler-Bernoulli beam that can be given by

$$\omega_n = \left(\frac{n\pi}{L}\right)^2 \sqrt{\frac{EI}{\rho A}} \quad (36)$$

ξ is the damping ratio that is defined as:

$$\xi = \frac{\alpha_e + \omega_n{}^2\alpha_i}{2\omega_n} = \xi_e + \xi_i \quad (37)$$

when $0 < \xi < 1$, the system is under-damped. In this case, the damped natural frequency can be generally rewritten as:

$$\omega_{nD} = \omega_n\sqrt{1 - \xi^2} \quad (38)$$

Table 1 compares the central deflection of the simply supported Euler–Bernoulli beam $(w(\frac{L}{2}, x_F)/w_{st})$ using the Green Function method along with the Fourier series solution [Foda and Abduljabbar, 1998]. It is seen that the results are fairly close. Based on results in Table 1, the central deflection of the Euler–Bernoulli beam $(w(\frac{L}{2}, x_F))$ is more sensitive to the variation of the speed parameter.

Table 1. The central deflection of the Euler–Bernoulli beam ($w(\frac{L}{2}, x_F)/w_{st}$) under a moving load

α	$\frac{X_F}{L}$	Present study	Foda and Abduljabbar [Foda and Abduljabbar, 1998]
0	0.1	0.296013	0.296
	0.3	0.792068	0.792
	0.5	1.00021	1.000
	0.7	0.792023	0.792
	0.9	0.296013	0.296
0.05	0.1	0.296763	0.296761
	0.3	0.793998	0.793997
	0.5	1.00247	1.00247
	0.7	0.793998	0.793997
	0.9	0.296763	0.296761
0.125	0.1	0.229522	0.226955
	0.3	0.689272	0.685135
	0.5	1.01565	1.01567
	0.7	0.920038	0.924161
	0.9	0.372143	0.374681
0.25	0.1	0.0736325	0.0653048
	0.3	0.995125	1.00021
	0.5	1.06571	1.06579
	0.7	0.695177	0.690039
	0.9	0.558959	0.567171
0.375	0.1	0.0347739	0.0274662
	0.3	0.676444	0.6687
	0.5	1.52377	1.53399
	0.7	1.0927	1.09811
	0.9	-0.0522479	-0.0648094

Figure 2 shows the two-dimensional contour graph of the forced vibration of the simply supported Euler-Bernoulli beam ($\frac{w\left(\frac{X_F}{L}, \frac{X_F}{L}\right)}{w_{st}}$) under moving load for different speed parameters α using Dynamic Green Function. The moving load is traversed from the start point on the left-hand side of the beam to the end point with constant speed. Figure 2 shows that the deflection of the beam under moving load is sensitive to the speed and position of the moving load. At the same time, the maximum deflection for the simply supported Euler-Bernoulli beam under moving load is approximately $w\left(\frac{X_F}{L}, \frac{X_F}{L}\right) = 1.58283 w_{st}$ in $\frac{X_F}{L} = 0.576735$ with the speed parameter 0.443. Figure 3 shows the influence of variation of the acceleration parameters a_{0x} on the deflections of the simply supported Euler–Bernoulli beam for a moving load with initial speed $v_{0x} = 0.10L$. It is shown that the acceleration plays an important role in the dynamic characteristics of the moving load problem.

From the curve for $a_{0x} = 0.5L$, the maximum deflection $w\left(\frac{X_F}{L}, \frac{X_F}{L}\right) = 0.98507\, w_{st}$ occurs when the load is located at X_F/L=0.40654, while for $a_{0x} = 0.1L$, the maximum deflection becomes $w\left(\frac{X_F}{L}, \frac{X_F}{L}\right) = 1.0268\, w_{st}$, when the load is located at X_F/L=0.58408

.

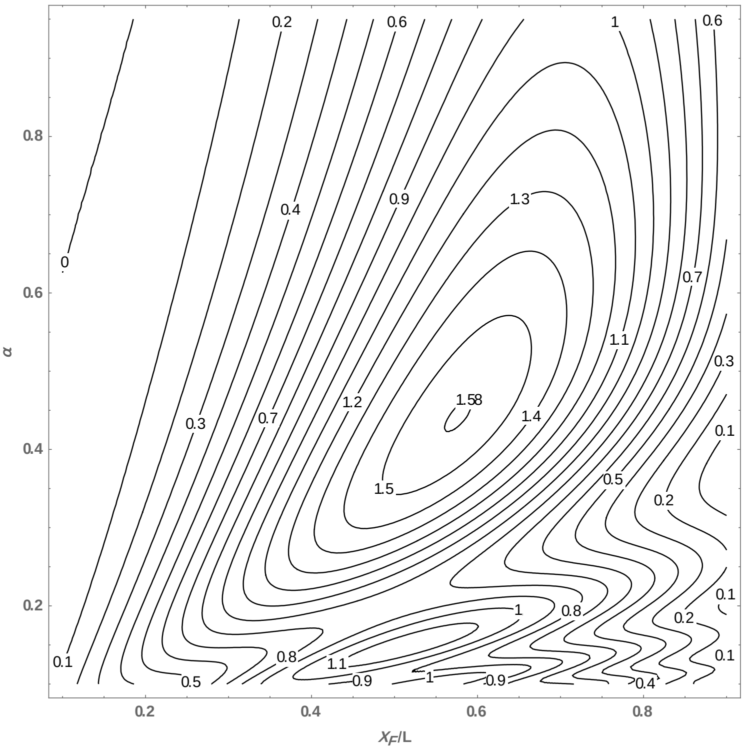

Figure 2. The forced vibration part of the deflection Euler-Bernoulli beam ($\frac{w\left(\frac{X_F}{L}, \frac{X_F}{L}\right)}{w_{st}}$) for different speed parameters α

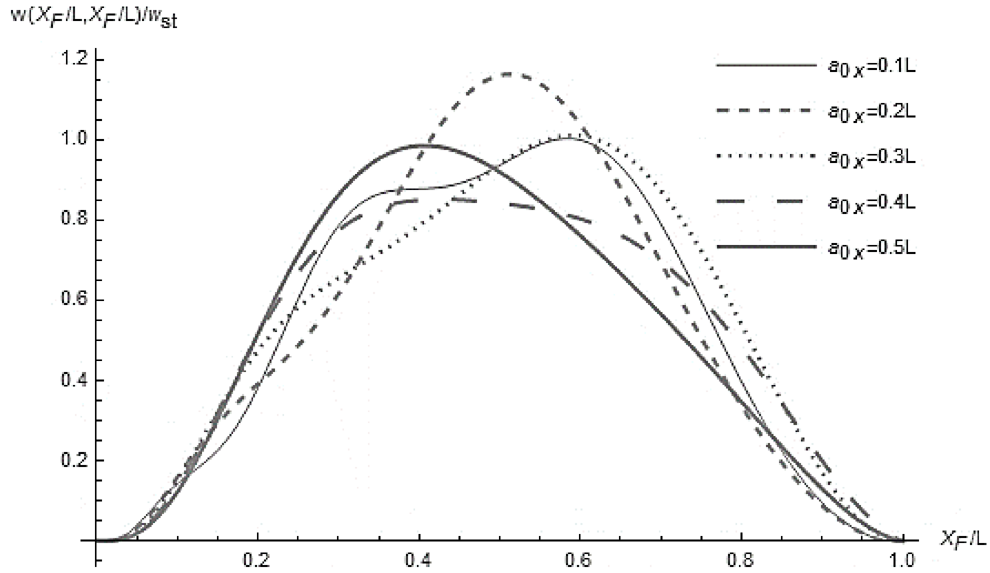

Figure 3. The forced vibration part of the deflection Euler-Bernoulli beam ($\frac{w\left(\frac{X_F}{L}, \frac{X_F}{L}\right)}{w_{st}}$) for different acceleration parameters a_{0x} of moving load ($v_{0x} = 0.10L$)

The two-dimensional contour graph of the simply supported Euler-Bernoulli beam ($\frac{w\left(\frac{X_F}{L},\frac{X_F}{L}\right)}{w_{st}}$) for an accelerating load with initial speed $v_{0x} = 0.15\text{L}$ and $v_{0x} = 0.90\text{L}$ are given in Figures 4 and 5, respectively. Figure 5 shows that the deflection curve shape tends to the left end when the acceleration decreases. Therefore, the maximum point of the deflection is depended on the increasing or decreasing acceleration. Also, the maximum deflection of the Euler-Bernoulli beam does not occur at the central point of the beam for all acceleration values. On the other hands, the acceleration value of load dominantly defines the dynamic deflection shape of the Euler-Bernoulli beam.

By applying the present method, the influence of the speed and acceleration of the moving load is evaluated vibration characteristics of the simply supported Euler-Bernoulli beam. For this purpose, the Euler-Bernoulli beam is assumed with characteristics as follows:

$K_W = 0.2\,\pi^4 \frac{EI}{L^2}$ $\qquad \xi_e = 0.10 \qquad \xi_i = 0.10$

$\phi^2 = \frac{\omega^2 \rho\, A}{EI} \qquad v = v_{0x} + a_{0x}t$

$X_F(t) = v_{0x}t + \frac{1}{2}a_{0x}t^2$

$\beta_R = \beta_L = 0 \qquad \beta_C = 1$

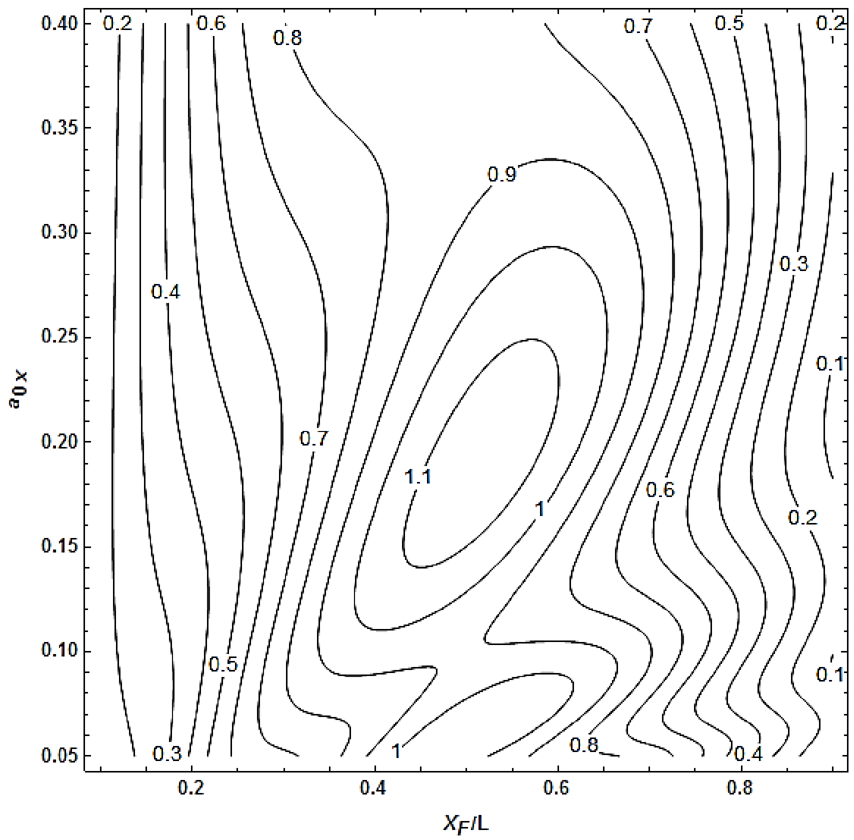

Figure 4. The forced vibration part of the deflection Euler-Bernoulli beam ($\frac{w\left(\frac{X_F}{L},\frac{X_F}{L}\right)}{w_{st}}$) for different acceleration parameters a_{0x} of moving load ($v_{0x} = 0.15\text{L}$)

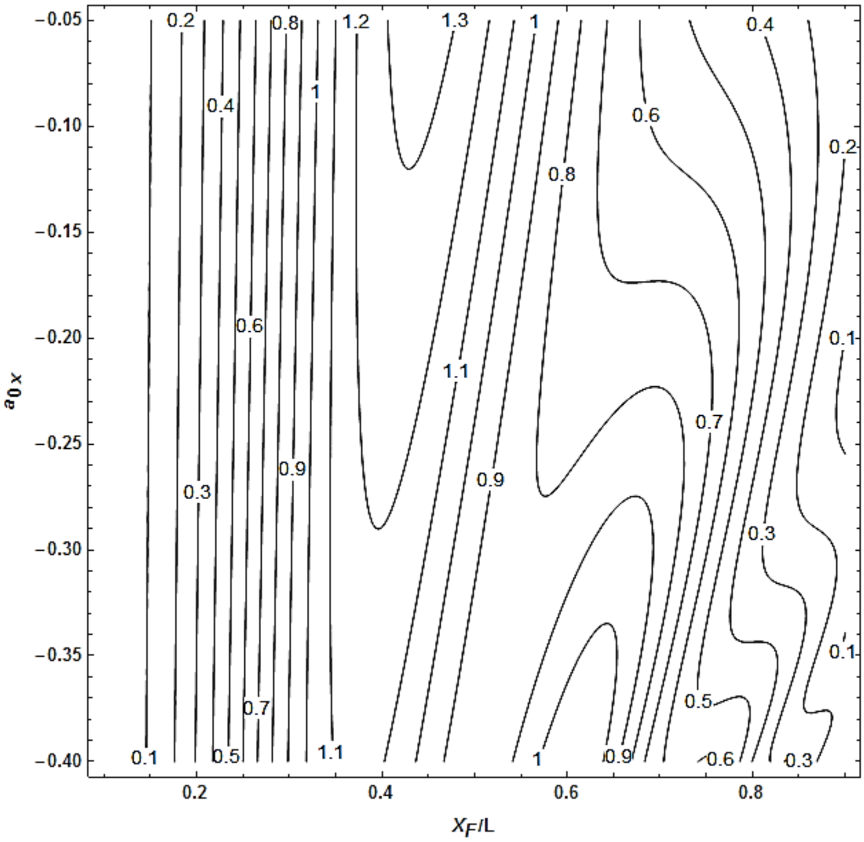

Figure 5. The forced vibration part of the deflection Euler-Bernoulli beam ($\frac{w\left(\frac{X_F}{L},\frac{X_F}{L}\right)}{w_{st}}$) for different acceleration parameters a_{0x} of moving load ($v_{0x} = 0.90L$)

Figure 6 shows the influence of variation of the acceleration parameters a_{0x} on the deflections of the damped Euler–Bernoulli beam for a moving load with initial speed $v_{0x} = 0.10L$. From the curve for $a_{0x} = 0.3L$, the maximum deflection $w\left(\frac{X_F}{L},\frac{X_F}{L}\right) = 0.811573\, w_{st}$ occurs when the load is located at $X_F/L=0.59383$, while for $a_{0x} = 0.1L$, the maximum deflection becomes $w\left(\frac{X_F}{L},\frac{X_F}{L}\right) = 0.812132\, w_{st}$, when the load is located at $X_F/L=0.59239$. The two-dimensional contour graph of the damped Euler-Bernoulli beam ($\frac{w\left(\frac{X_F}{L},\frac{X_F}{L}\right)}{w_{st}}$) for a accelerating load with initial speed $v_{0x} = 0.15L$ and $v_{0x} = 0.90L$ are given in Figures 7 and 8, respectively. In addition, the influence of the elastic coefficient of Winkler foundation is evaluated vibration characteristics of the simply supported Euler-Bernoulli beam under accelerated moving load. For this purpose, the Euler-Bernoulli beam is assumed with characteristics as follows:

$$K_W = 0.1\,\pi^4 \frac{EI}{L^2} - 0.5\,\pi^4 \frac{EI}{L^2} \qquad \xi_e = 0.10 \qquad \xi_i = 0$$

$$\phi^2 = \frac{\omega^2 \rho A}{EI} \qquad \frac{v}{L} = v_{0x} + a_{0x} t \quad X_F(t) = v_{0x} t + \frac{1}{2} a_{0x} t^2$$

$$v_{0x} = 0.10L \qquad \beta_L = 0 \qquad \beta_C = \beta_R = 1/2$$

Table 2 compares the deflection of the simply supported Euler–Bernoulli beam ($w(0.6L, X_F)/w_{st}$) under moving load with $a_{0x} = 0.1L, 0.2L$ on the partial elastic foundation.

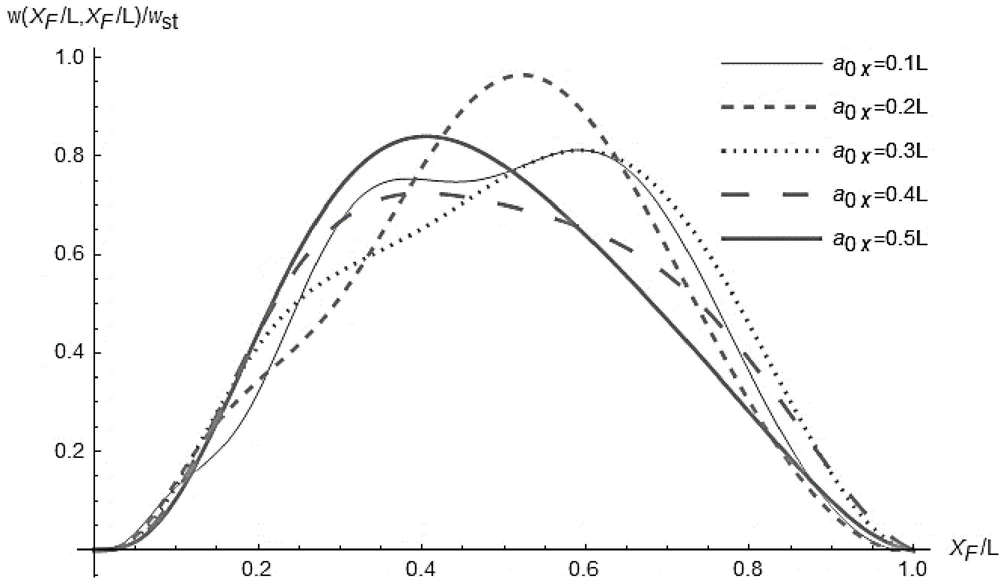

Figure 6. The forced vibration part of the deflection of the damped Euler-Bernoulli beam ($\frac{w\left(\frac{X_F}{L},\frac{X_F}{L}\right)}{w_{st}}$) for different acceleration parameters a_{0x} of moving load ($v_{0x} = 0.10L$)

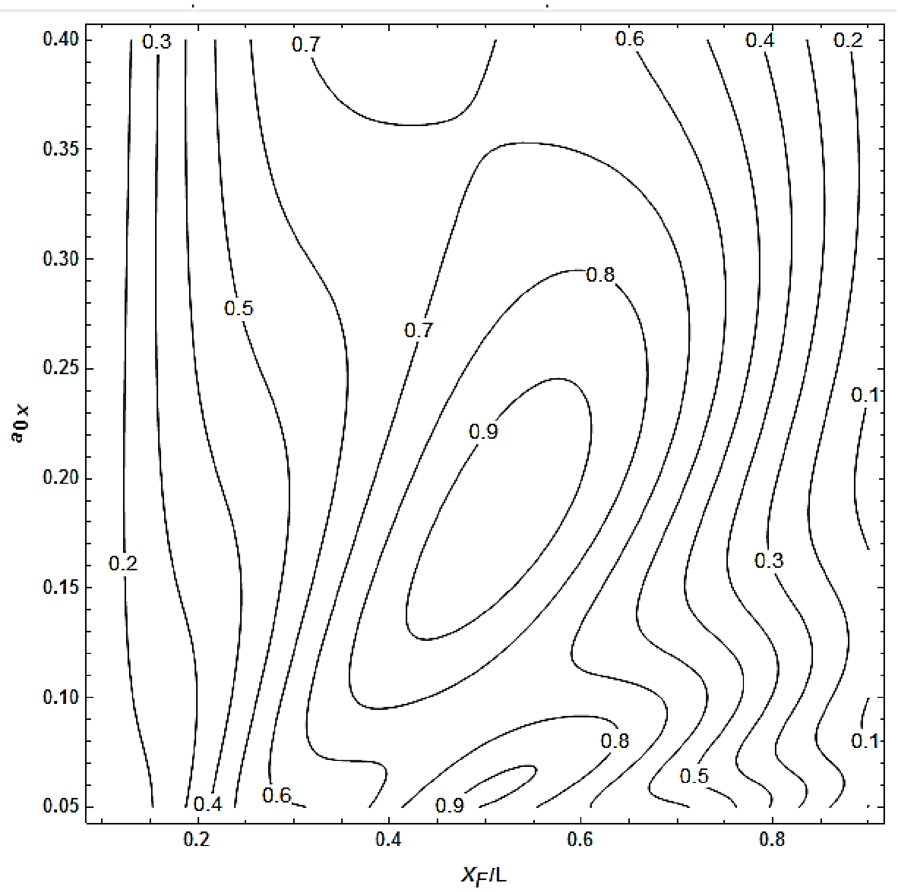

Figure 7. The forced vibration part of the deflection of the damped Euler-Bernoulli beam ($\frac{w\left(\frac{X_F}{L},\frac{X_F}{L}\right)}{w_{st}}$) for different acceleration parameters a_{0x} of moving load ($v_{0x} = 0.15L$)

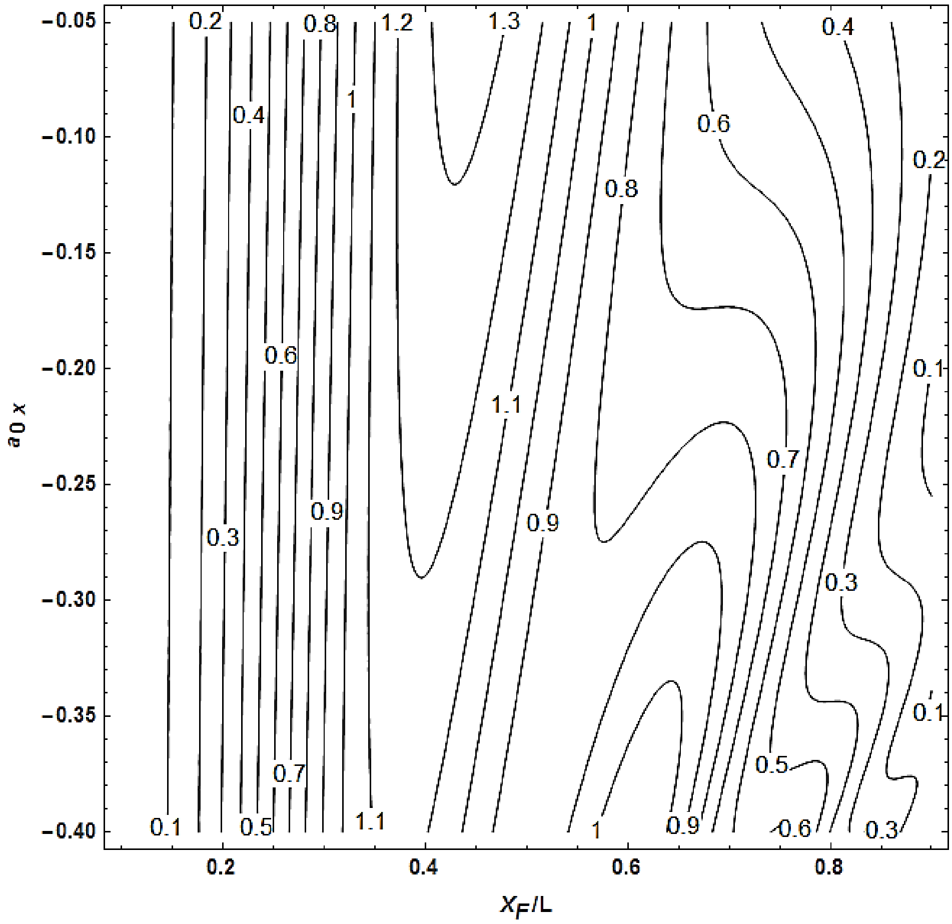

Figure 8. The forced vibration part of the deflection of the damped Euler-Bernoulli beam ($\frac{w\left(\frac{X_F}{L},\frac{X_F}{L}\right)}{w_{st}}$) for different acceleration parameters a_{0x} of moving load ($v_{0x} = 0.90L$)

Table 2 presents that the deflection of the Euler–Bernoulli beam is more sensitive to the variation of the elastic coefficient of Winkler foundation. Figure 9 shows the influence of variation of the elastic coefficient of Winkler foundation on the deflections of the damped Euler–Bernoulli beam for a moving load with initial accelerate $a_{0x} = 0.10$L.

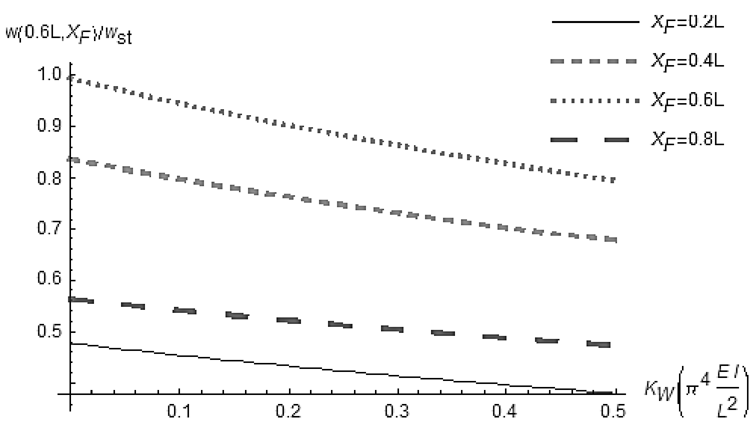

Figure 9. The forced vibration part of the deflection of the damped Euler-Bernoulli beam ($\frac{w(0.6L,X_F)}{w_{st}}$) for different elastic coefficient of Winkler foundation ($a_{0x} = 0.1$L)

Table 2. The deflection of the Euler–Bernoulli beam ($w(0.6L, X_F)/w_{st}$) under a moving load on partial elastic foundation

K_W	$\frac{X_F}{L}$	$a_{0x} = 0.1L$	$a_{0x} = 0.2L$
0	0.1	0.294147	0.326731
	0.3	0.798037	0.633518
	0.5	0.882019	1.08782
	0.7	0.899351	0.784643
	0.9	0.18823	0.155375
$0.1\,\pi^4 \frac{EI}{L^2}$	0.1	0.276366	0.305222
	0.3	0.752305	0.606656
	0.5	0.846282	1.02883
	0.7	0.854809	0.753439
	0.9	0.189359	0.16046
$0.2\,\pi^4 \frac{EI}{L^2}$	0.1	0.260277	0.285768
	0.3	0.710928	0.582368
	0.5	0.813958	0.975507
	0.7	0.814517	0.725257
	0.9	0.190394	0.165076
$0.3\,\pi^4 \frac{EI}{L^2}$	0.1	0.24565	0.268087
	0.3	0.673312	0.560303
	0.5	0.784581	0.927072
	0.7	0.777893	0.699676
	0.9	0.191346	0.169288
$0.4\,\pi^4 \frac{EI}{L^2}$	0.1	0.232295	0.251949
	0.3	0.638967	0.54017
	0.5	0.757765	0.882881
	0.7	0.744454	0.676353
	0.9	0.192226	0.173147
$0.5\,\pi^4 \frac{EI}{L^2}$	0.1	0.220053	0.237158
	0.3	0.607482	0.521727
	0.5	0.733189	0.842395
	0.7	0.713801	0.654999
	0.9	0.193043	0.176698

4. Conclusions

This paper presents the Dynamic Green Function for the vibration of the damped Euler-Bernoulli beam on the partial Winkler foundation under accelerated moving load. The method of Green functions is efficient when compared with other methods. The Green function yields exact solutions in closed forms. At the same time, the boundary conditions are embedded in the Green functions by the Green function method. The effect of the elastic coefficient of Winkler foundation, velocity and accelerate of load are determined. Finally, some numerical examples are shown to illustrate the efficiency of the new formulation based on the Dynamic Green Function.

5. Acknowledgments

The work was supported by the University of Mohaghegh Ardabili (reference number:1283).

6. References

-Abu-Hilal, M. (2003) "Forced vibration of Euler–Bernoulli beams by means of dynamic Green functions", Journal of Sound and Vibration, Vol. 267, No. 2, pp. 191-207.

-Bajer, C. I.and Dyniewicz, B. (2012) "Numerical analysis of vibrations of structures under moving inertial load", Springer.

-Beskou, N. D.and Theodorakopoulos, D. D. (2011) "Dynamic effects of moving loads on road pavements: a review", Soil Dynamics and Earthquake Engineering, Vol. 31, No. 4, pp. 547-567.

-Dimitrovová, Z. (2016) "Critical velocity of a uniformly moving load on a beam supported by a finite depth foundation", Journal of Sound and Vibration, Vol. 366, pp. 325-342.

-Dimitrovová, Z.and Rodrigues, A. F. S. (2012) "Critical velocity of a uniformly moving load", Advances in Engineering Software, Vol. 50, pp. 44-56.

-Esmaeili, M., Mohammadzadeh, S. and Mehrali, M. (2016) "Dynamic response of the coupled vehicle-floating slab track system using finite element method", International Journal of Transportation Engineereing, Vol. 4, No. 1, pp. 9-26.

-Foda, M. A. and Abduljabbar, Z. (1998) "A dynamic green function formulation for the response of a beam structure to a moving mass", Journal of Sound and Vibration, Vol. 210, No. 3, pp. 295-306.

-Ghannadiasl, A. and Mofid, M. (2014) "Dynamic green function for response of timoshenko beam with arbitrary boundary conditions", Mechanics Based Design of Structures and Machines, Vol. 42, No. 1, pp. 97-110.

-Ghannadiasl, A.and Mofid, M. (2015) "An analytical solution for free vibration of elastically restrained Timoshenko beam on an arbitrary variable Winkler foundation and under axial load", Latin American Journal of Solids and Structures, an ABCM Journal, Vol. 12, No. 13, pp. 2417-2438.

-Gładysz, M. and Śniady, P. (2009) "Spectral density of the bridge beam response with uncertain parameters under a random train of moving forces", Archives of Civil and Mechanical Engineering, Vol. 9, No. 3, pp. 31-47.

-Hamada, T. (1981) "Dynamic analysis of a beam under a moving force: a double Laplace transform solution", Journal of Sound and Vibration, Vol. 74, No. 2, pp. 221-233.

-Hilal, M. A. and Zibdeh, H. S. (2000) "Vibration analysis of beams with general boundary conditions traversed by a moving force", Journal of Sound and Vibration, Vol. 229, No. 2, pp. 377-388.

-Kargarnovin, M. and Younesian, D. (2004) "Dynamics of Timoshenko beams on Pasternak foundation under moving load", Mechanics Research Communications, Vol. 31, No. 6, pp. 713-723.

-Koziol, P.and Mares, C. (2010) "Wavelet approach for vibration analysis of fast moving load on a viscoelastic medium", Shock and Vibration, Vol. 17, No. 4, pp. 461-472.

-Lancaster, P. and Shkalikov, A. (1994) "Damped vibrations of beams and related spectral problems", Canadian Applied Mathematics Quarterly, Vol. 2, No. 1, pp. 45-90.

-Li, X. Y., Zhao, X. and Li, Y. H. (2014) "Green's functions of the forced vibration of Timoshenko beams with damping effect", Journal of Sound and Vibration, Vol. 333, No. 6, pp. 1781-1795.

-Lin, Y.-H. (1994) "Vibration analysis of Timoshenko beams traversed by moving loads", Journal of Marine Science and Technology, Vol. 2, No. 4, pp. 25-35.

-Mackertich, S. (1990) "Moving load on a Timoshenko beam", The Journal of the Acoustical Society of America, Vol. 88, No. 2, pp. 1175-1178.

-Mehri, B., Davar, A. and Rahmani, O. (2009) "Dynamic green function solution of beams under a moving load with different boundary conditions", Scientia Iranica, Vol. 16, No. 3, pp. 273-279.

-Mohammadzadeh, S. and Mosayebi, S. A. (2014) "Dynamic analysis of axially beam on visco-elastic foundation with elastic supports under moving load", International Journal of Transportation Engineereing, Vol. 2, No. 4, pp. 289-296.

-Ouyang, H. (2011) "Moving-load dynamic problems: A tutorial (with a brief overview)", Mechanical Systems and Signal Processing, Vol. 25, No. 6, pp. 2039-2060.

-Savin, E. (2001) "Dynamic amplification factor and response spectrum for the evaluation of vibrations of beams under successive moving loads", Journal of Sound and Vibration, Vol. 248, No. 2, pp. 267-288.

-Wang, C. (1995) "Timoshenko beam-bending solutions in terms of Euler-Bernoulli solutions", Journal of Engineering Mechanics, Vol. 121, No. 6, pp. 763-765.

-Zakeri, J. and Shahbabaei, M. (2015) "Investigation on effect of elastic supports stiffness on natural frequencies and modes of two span beams under free vibration", Quarterly Journal of Transportation Engineering, Vol. 7, No. 1, pp. 45-54.

-Zrnić, N., Gašić, V. and Bošnjak, S. (2015) "Dynamic responses of a gantry crane system due to a moving body considered as moving oscillator", Archives of Civil and Mechanical Engineering, Vol. 15, No. 1, pp. 243-250.